Molecular Cell, Vol. 18, 185–200, April 15, 2005, Copyright ©2005 by Elsevier Inc. DOI 10.1016/j.molcel.2005.03.017

Sororin, a Substrate of the Anaphase-Promoting Complex, Is Required for Sister Chromatid Cohesion in Vertebrates

Susannah Rankin,[1,*] Nagi G. Ayad,[1,2] and Marc W. Kirschner[1]
[1]Systems Biology Department
Department of Cell Biology
Harvard Medical School
Boston, Massachusetts 02115

Summary

We have identified a regulator of sister chromatid cohesion in a screen for cell cycle-controlled proteins. This 35 kDa protein is degraded through anaphase-promoting complex (APC)-dependent ubiquitination in G1. The protein is nuclear in interphase cells, dispersed from the chromatin in mitosis, and interacts with the cohesin complex. In *Xenopus* embryos, overexpression of the protein causes failure to resolve and segregate sister chromatids in mitosis and an increase in the level of cohesin associated with metaphase chromosomes. In cultured cells, depletion of the protein causes mitotic arrest and complete failure of sister chromatid cohesion. This protein is thus an essential, cell cycle-dependent mediator of sister chromatid cohesion. Based on sequence analysis, this protein has no apparent orthologs outside of the vertebrates. We speculate that the protein, which we have named *sororin*, regulates the ability of the cohesin complex to mediate sister chromatid cohesion, perhaps by altering the nature of the interaction of cohesin with the chromosomes.

Introduction

Sister chromatid cohesion is essential for the proper segregation of newly replicated chromosomes at anaphase. Cohesion opposes the poleward tension upon which the spindle assembly checkpoint relies to signal bipolar attachment of the chromosomes (Tanaka et al., 2000). Both sister chromatid cohesion and its resolution at anaphase are tightly coupled to cell cycle progression, which in turn is controlled through the orderly and interdependent activation and inactivation of kinases, phosphatases, and E3 ligases (reviewed in Reed [2003]). Numerous proteins mediate sister chromatid cohesion, although the exact mechanism is not clear. These include cohesin, a multisubunit complex consisting of a heterodimer of SMC proteins and two additional proteins, Scc1 (also referred to as Mcd1 or Rad21 in other systems) and Scc3 (reviewed in Hirano [2002]). In addition to the cohesin complex, sister chromatid cohesion requires the activities of Pds5, a protein that is loosely associated with cohesin (Hartman et al., 2000; Panizza et al., 2000; Sumara et al., 2000), and Ctf7/Eco1, an acetyl transferase (Ivanov et al., 2002; Skibbens et al., 1999; Toth et al., 1999). In yeast, a dimeric complex containing Scc2 and Scc4 is essential for cohesin loading onto the chromatin but dispensable once cohesion is established (Ciosk et al., 2000); similar activities have recently been characterized in vertebrates (Gillespie and Hirano, 2004; Takahashi et al., 2004). Recently, a protein related to the TIMELESS clock protein of *Drosophila* has been shown to interact with cohesin and regulate cohesion in metazoans (Chan et al., 2003).

In addition to its role in chromosome segregation, sister chromatid cohesion plays an important role in DNA repair. This may reflect the need for the replicated strands to be in proximity to each other to serve as templates for homologous recombination and repair. In several systems, the proteins essential for sister chromatid cohesion have been shown to play a role in DNA damage repair. In fact, the cohesin regulatory subunit Scc1, whose cleavage initiates sister chromatid separation (Uhlmann et al., 1999), was originally identified in a screen for genes involved in radiation sensitivity (Birkenbihl and Subramani, 1992; Phipps et al., 1985). Recent work has also established a connection between the kinase that transduces the DNA damage signal and Smc1, one of the subunits of cohesin (Kim et al., 2002; Kitagawa et al., 2004; Yazdi et al., 2002).

Several lines of evidence suggest that sister chromatid cohesion is established during S phase, and this of course makes mechanistic sense, because newly replicated sister strands are necessarily close to each other by virtue of their proximity to the replication fork and are thus easily bound together at this time. It is known that the Scc1/Rad21 subunit of the core cohesin complex must be present during S phase for the establishment of cohesion (Uhlmann and Nasmyth, 1998) and that certain mutants defective in sister chromatid cohesion can be suppressed by the overexpression of components of the DNA replication machinery (Skibbens et al., 1999). In addition, the establishment of sister chromatid cohesion requires the activity of a particular DNA polymerase (Wang et al., 2000). Although some proteins, such as the cohesin complex itself, are essential to both to establish and maintain cohesion (Uhlmann and Nasmyth, 1998), others such as Scc2, Scc4, and Ecol/Ctf7 are dispensable once replication is complete (Ciosk et al., 2000; Skibbens et al., 1999).

In order for the events of mitosis to unfold properly, the relative timing of each step must be tightly controlled. In several cases, this control is exerted through proteolysis of key regulatory molecules. At the metaphase to anaphase transition, the APC, a multisubunit E3 ubiquitin ligase, is sequentially activated by two adaptor proteins, Cdc20 and Cdh1, which confer substrate specificity on the complex (reviewed in Reed [2003]). Substrates of this complex include the cyclins, mitotic kinases, and the anaphase inhibitor securin. The limited number of known substrates, and the critical roles that they play in controlling mitosis, suggested that the identification and characterization of additional substrates would be valuable. We were particularly in-

*Correspondence: susannah_rankin@hms.harvard.edu
[2]Present address: Department of Biomedical Research, The Scripps Research Institute, Jupiter, Florida 33458.

terested in finding the substrates of Cdh1-activated APC (APC^{Cdh1}), which is activated after the initiation of anaphase and remains active into G1 phase. We reasoned that this class of substrates might include novel downstream effectors of the cell division cycle. We have screened for APC^{Cdh1} substrates by in vitro expression cloning (King et al., 1997; Lustig et al., 1997) and identified a regulator of sister chromatid cohesion. This 35 kDa protein interacts with cohesin and is essential for proper sister chromatid cohesion. In addition, we show that overexpression of the protein causes a cohesion defect in chromosomes assembled in vitro. Our data suggest that this protein is a positive regulator of cohesion and that it ensures maintenance of sister chromatid cohesion in metaphase.

Results

Identification of p35, a Substrate of APC^{cdh1}

Supplementation of *Xenopus* interphase egg extracts with recombinant Cdh1 protein causes activation of the APC and leads to ubiquitination and subsequent instability of Cdh1-dependent APC substrates (Fang et al., 1998b). Based on this observation, we used a modification of screens done previously (Lustig et al., 1997; McGarry and Kirschner, 1998; Stukenberg et al., 1997) to identify substrates of Cdh1-activated APC. Briefly, small pools of in vitro-transcribed and -translated, ^{35}S-labeled proteins were incubated in interphase egg extracts either with or without supplementation with recombinant Cdh1. Proteins that were unstable in the presence of Cdh1 were identified after sodium dodecylsulfate polyacrylamide gel electrophoresis (SDS-PAGE), and plasmids encoding these proteins were isolated from the relevant pools and sequenced. We identified one cDNA, reported previously, which encoded a protein involved in regulation of the G2/M transition (Ayad et al., 2003). A second cDNA encoded a protein of an apparent molecular weight of 35 kDa, hereafter referred to as p35. As shown in Figure 1A (top), and consistent with the design of the screen, *Xenopus* p35 (Xp35) is stable in interphase egg extracts and degraded in extracts supplemented with Cdh1. When nondegradable cyclin is added, the extract is driven into a metaphase/anaphase-like state in which APC^{Cdc20} is active. Under these conditions, the mobility of p35 is reduced due to mitotic phosphorylation (data not shown), though the protein level remains unchanged. These data are similar to those obtained with Cdc20, a previously characterized substrate of APC^{Cdh1} (Fang et al., 1998a; Prinz et al., 1998) (Figure 1A, middle), and are in contrast to cyclin B, which is a substrate both of APC^{Cdc20} and APC^{cdh1} (Fang et al., 1998b) (Figure 1A: bottom).

The plasmid containing the *Xenopus* p35 gene was sequenced and shown to encode an uncharacterized protein that is conserved among vertebrates. The alignment of the *Xenopus* protein with homologous proteins from other species is shown in Figure 1C. In addition to the proteins shown in Figure 1, we have found expressed sequence tags (ESTs) encoding homologous proteins from a number of other vertebrate species, including pig, cow, and zebrafish. We are unable to find evidence of a conserved protein in nonvertebrates. It is possible that the function of p35 is particular to vertebrates. Alternatively, the sequences of orthologous proteins in nonvertebrates may not be conserved enough to be easily identified based on homology. A precedent for this is found in another APC substrate, the cell cycle regulator Pds1/Cut2, which, although not conserved at the protein level, appears to be well conserved in terms of biochemical function (Yamamoto et al., 1996; Zou et al., 1999). The human p35 gene was previously identified in a metaanalytical expression screen to identify genes that are coregulated with known cell cycle genes, including CDK1, cyclin B, and the BUB1 (Walker, 2001), suggesting that p35 might have a cell cycle function.

The amino acid sequence for p35 shows no previously characterized functional domains. The protein is very basic, with calculated pIs ranging from 9.7 to 10.3, depending on the species. The protein is most basic at the N terminus (amino acids 1–100 of human p35 have a calculated pI of 11.76). Orthologs are most conserved at their extreme C termini, with an additional small conserved domain near the middle of the protein (see Figure 1C). It has previously been shown that Cdh1-dependent APC substrates contain specific recognition sequences that target them for ubiquitination by APC, leading to their subsequent degradation (King et al., 1996; Pfleger and Kirschner, 2000). We scanned the protein sequence of p35 and found a "KEN box," which in other proteins has been shown to be sufficient to trigger APC^{Cdh1}-dependent ubiquitination, as well as several potential "destruction boxes" (D boxes). As seen in Figure 1B, mutation of the sequence K-E-N to A-A-A in Xp35 completely stabilized the protein in Cdh1-supplemented extracts over the time course of the experiment, whereas mutation of two other potential D boxes (Figure 1C) had no effect on the stability of the protein (data not shown). Supplementation of the extracts with an N-terminal fragment of cyclin B, which acts as a competitive substrate for the APC ubiquitination machinery, also stabilized the protein (data not shown). The data in Figure 1 confirm that we have identified a substrate of the APC and demonstrate that it is a substrate only when the complex is activated by Cdh1, not by Cdc20.

p35 Is Similarly Regulated in Somatic Cells

We generated antibodies against the human and mouse orthologs of p35. The human and mouse p35 genes were cloned, expressed as a glutathione S-transferase (GST) fusions in *E. coli*, and these fusions were injected into mice. A panel of monoclonal antibodies was generated. One monoclonal antibody, 2E10, recognized both human and mouse recombinant proteins in immunoblots and by immunolocalization in cells expressing the genes from transfected plasmids (data not shown). This antibody also recognized a 35 kDa band, sometimes seen as a doublet, in both human and murine cell extracts, as shown in Figure 2A.

We next wanted to determine whether p35 protein levels fluctuate with the cell cycle in somatic cells. HeLa cells were synchronized by double thymidine arrest, released, and collected at various times after release. In addition, the microtubule poison nocodazole was added to the culture 5 hr after the release from double thymidine arrest to activate the spindle check-

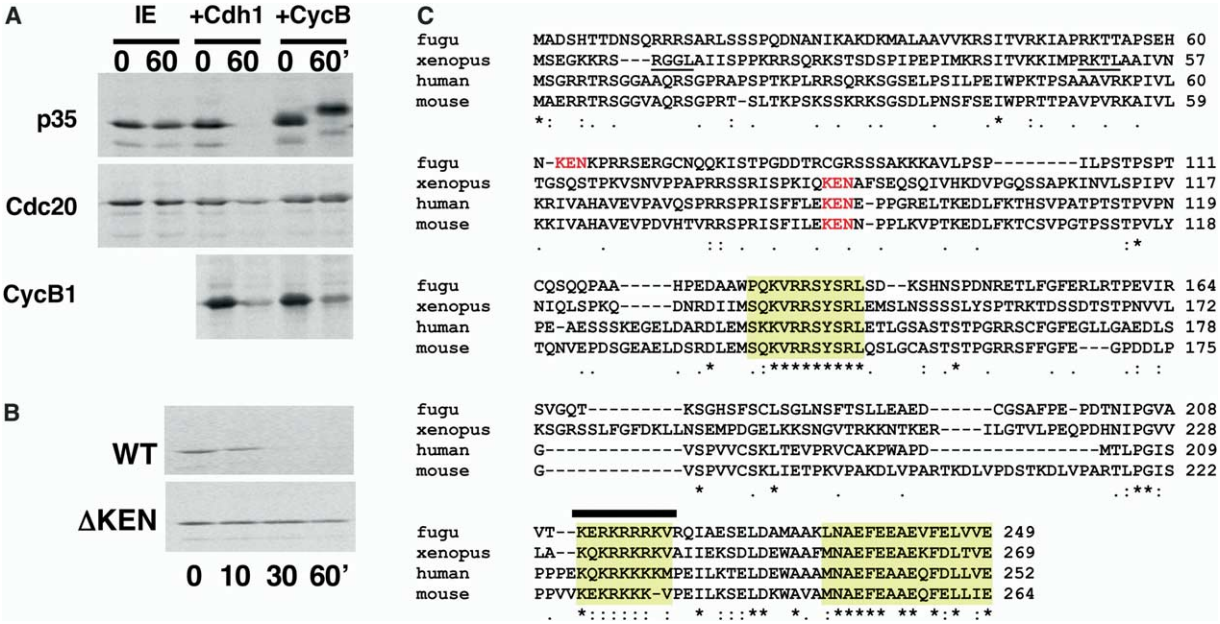

Figure 1. Identification of p35

(A) In vitro-translated ^{35}S-labeled *Xenopus* p35 (top), cdc20 (middle), and cyclin B (bottom panel) were added to interphase egg extract (IE), interphase extract supplemented with recombinant Cdh1 (+Cdh1), or extract driven into mitosis by the addition of recombinant nondegradable cyclin B protein (+CycB). Samples were collected at 0 and 60 min and analyzed by SDS-PAGE. (The first two lanes are omitted from the bottom panel, because cyclin B drives interphase extracts into mitosis.)

(B) Mutation of K-E-N to A-A-A in *Xenopus* p35 stabilizes the protein in extracts supplemented with Cdh1. In vitro-translated ^{35}S-labeled wild-type (wt) (top) or KEN box mutants (bottom) of p35 were incubated in interphase extracts supplemented with Cdh1, and samples were collected at the times indicated (in minutes) and analyzed by SDS-PAGE.

(C) Alignment of predicted p35 proteins from various organisms. Shown is the Clustal W alignment of p35 orthologs, identified by homology with *Xenopus* p35, from several organisms. Invariant residues are indicated by an asterisk (*), whereas conserved residues are indicated by a colon (:), and semiconserved residues are indicated by a period (.). Domains that are particularly well conserved are highlighted in yellow. KEN boxes are shown in red, and a putative NLS sequence is overlined. Two potential D boxes that were mutated and shown to have no effect on the stability of xp35 are underlined. The amino acid numbers of each protein are shown at the right hand side of the alignment. Genbank accession numbers for the proteins are: *Xenopus*, AAX73201; human, NP_542399; and mouse, NP_080686. The Fugu fish protein sequence was obtained through the BLAST genomes server at NCBI and is identified as FuguGenscan_24141. For simplicity, only one of two very similar *Xenopus* genes is shown.

point and prevent exit from mitosis. As shown in Figure 2B, p35 levels are consistent after release from double thymidine arrest. Occasionally, we do see an increase in p35 levels as cells progress through S phase; we believe this variability reflects imperfect reproducibility in synchronization protocols. As cells enter mitosis, the mobility of the protein is reduced due to mitotic phosphorylation, and the protein levels remain relatively stable. In contrast, when cells arrested in mitosis (by sequential treatment with thymidine and nocodazole) are released into interphase, the levels of p35 drop dramatically. As shown in Figure 2C, p35 levels decrease at concomitant with the loss of cyclin B and coincident with the mobility shift in the APC subunit Cdc27, which is known to have retarded mobility in mitosis. The results in Figures 2B and 2C are consistent with the notion that the level of p35 is controlled in somatic cells, at least in part, by APC^{cdh1} as suggested by our experiments in embryonic extracts (Figure 1).

p35 Is Nuclear in Interphase and Cytosolic in Mitosis

In immunofluorescence experiments, both human and mouse cells showed similar patterns of protein distribution. In the examples shown in Figures 3A and 3B, asynchronously growing mouse NIH-3T3 cells were stained with an anti-p35 monoclonal antibody. Cells in interphase show varying amounts of punctate nuclear staining (some with little or no detectable staining), whereas mitotic cells show diffuse staining throughout the cell. In contrast to the staining seen in interphase cells, there was no apparent concentration of p35 staining on chromatin in mitotic cells. The staining in mitotic cells was diffuse and cytoplasmic, noticeably more intense than the cytoplasmic signal in interphase cells (compare the cytoplasmic signal of the anaphase cell in Figure 3B with that of the adjacent interphase cell). Based on DAPI counterstaining, p35 staining was no longer limited to the nucleus once DNA condensation had begun. A similar protein distribution was observed when a plasmid encoding a Myc-tagged version of p35 was immunostained with anti-Myc antibodies (data not shown). The pattern of p35 localization as cells proceed through the cell cycle suggested that p35 dispersal from the chromatin might occur at the G2-M transition, perhaps as a result of phosphorylation or some other mitotically controlled event.

The apparent dispersal of p35 from the nuclei/chromatin at the G2/M transition was confirmed by fraction-

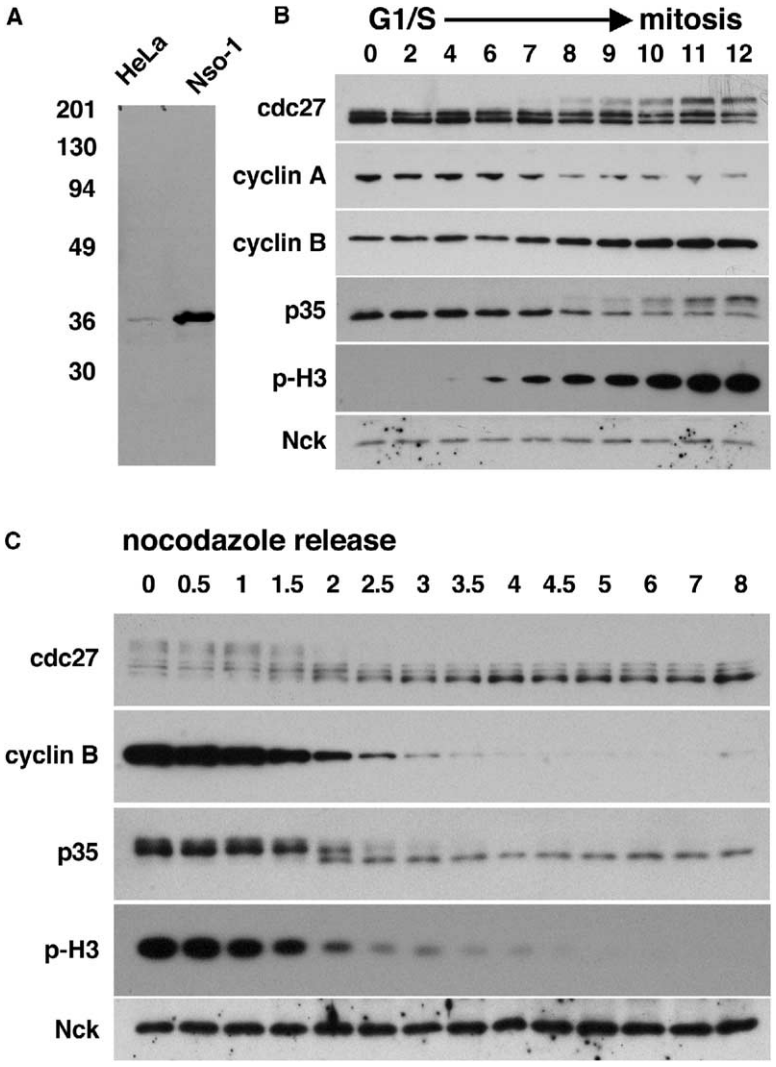

Figure 2. Cell Cycle Profile of p35 Expression in Somatic Cells

(A) Immunoblot of p35 protein in somatic cell extracts. Monoclonal antibody 2E10 was used to blot against total cell lysates from human and mouse cells. A single major band of ~35 kDa is detected in each case.

(B) Analysis of p35 levels in G1/S through mitosis. HeLa cells were synchronized by double thymidine arrest and released at t = 0. Nocodazole was added at 5 hr to prevent mitotic exit. Samples were collected at the times indicated after release and immunoblotted for p35. Also shown are immunoblots of the same fractions against Cdc27, cyclin B, cyclin A, phosphorylated histone H3, and Nck (as a loading control).

(C) Levels of p35 decrease after release from mitosis. Cells arrested in mitosis by sequential thymidine and nocodazole treatment were collected at the indicated times after nocodazole washout and immunoblotted against p35, cyclin B, Cdc27, and phosphorylated-histone H3. The samples were also immunoblotted for Nck as a loading control. (Note: antiphosphohistone and anticyclin A blots were performed on separate gels with comparable loading controls.)

ation of synchronized cells as they entered mitosis into soluble and chromatin-associated proteins. HeLa S3 cells were synchronized by double thymidine arrest and release, and nocodazole was added to prevent subsequent mitotic exit. Samples were collected at various times after release, and the cells were lysed and separated into crude nuclear and cytosolic fractions, which were then immunoblotted for p35. The fractions were also probed for topoisomerase IIα, which is constitutively associated with the chromatin and thus serves as a marker of cellular fractionation, as well as N-WASP, a ubiquitous protein involved in regulation of actin assembly (as a loading control). The blots were also probed for Smc3, a nuclear protein released from chromatin in prophase. As seen in Figure 3C, p35 was associated with the nuclear pellet over the course of S phase after release from thymidine arrest. As the cells began to enter mitosis, p35 was phosphorylated, and this lower mobility species was no longer associated with the nuclear pellet. This result is consistent with the observation made in the immunofluorescence experiments in which the p35 signal became diffuse in the cytoplasm at the G2/M transition. It is possible that a small fraction of p35 remains associated with mitotic chromosomes, but our results suggest that the majority is released into a soluble fraction on mitotic entry, coincident with the mobility shift in the protein. Consistent with this, we are unable to detect p35 on mitotic chromosomes by immunofluorescence.

p35 Interacts with Cohesion Proteins

In interphase cells, p35 is very tightly associated with the nuclei, and we were unable to isolate it associated with other components. When released from interphase nuclei by nuclease digestion, p35 was not associated with other proteins, and in extracts prepared from mitotic cells, the soluble p35 was monomeric based on gel-filtration analysis and thus provided no insight into the function of the protein (data not shown). In an attempt to identify interacting proteins that might provide information about p35 function, we used recombinant p35 as an affinity reagent. As p35 is predominantly nuclear, we reasoned that nuclear extracts would provide a good starting material in searching for p35-interacting pro-

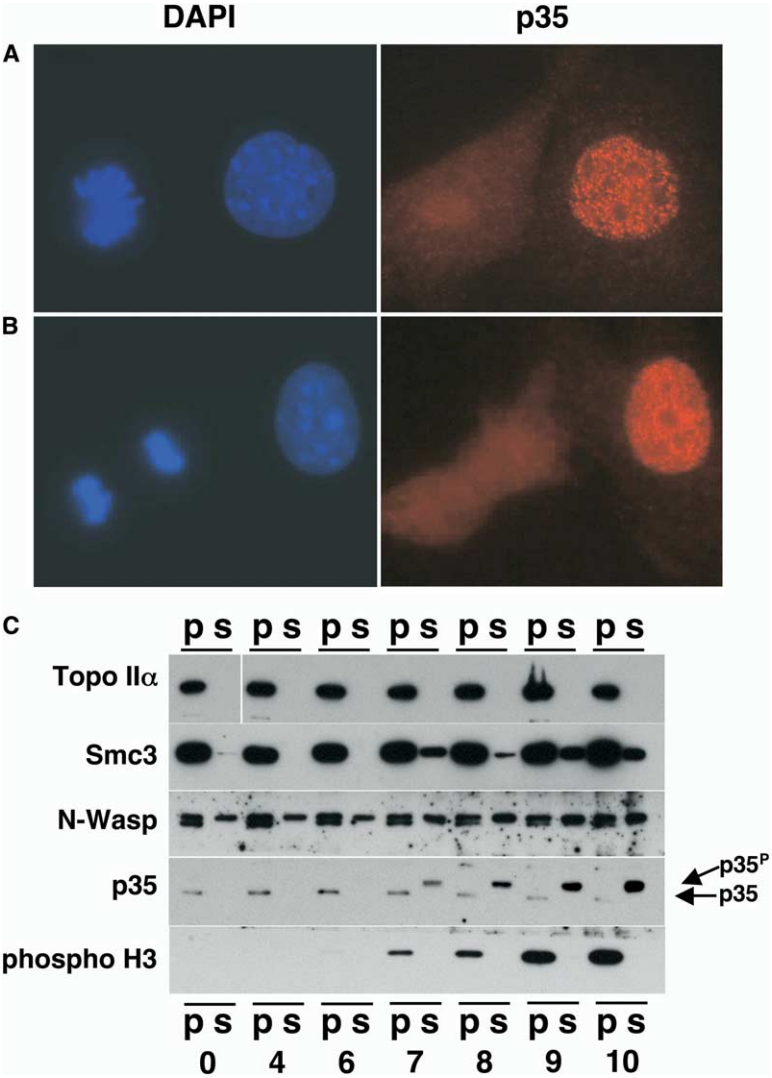

Figure 3. p35 Is Nuclear in Interphase, Cytosolic in Mitosis

(A and B) Mouse cells immunostained for p35 show both nuclear speckles and ground staining in interphase and diffuse cytoplasmic staining in mitosis. Each image contains two cells: one mitotic and another in interphase. The metaphase cell in (A) as well as the late anaphase cell in (B) show diffuse cytoplasmic staining for p35. In contrast, the interphase cells in both cases show numerous nuclear speckles.

(C) Lysates from synchronously growing HeLa cells arrested by double thymidine block and release were separated into nuclear pellets (p) and cytosolic supernatant (s) fractions, and each was blotted for p35 (bottom). In addition, the same samples were blotted for topoisomerase IIα and Smc3 as markers of cellular fractionation and N-WASP as a loading control. As seen previously, the reduced mobility of p35 in the late time points reflects mitotic phosphorylation of the protein. The slower migrating, mitotically phosphorylated version of p35 is consistently in the supernatant fraction. In contrast, topoisomerase IIα is quantitatively pelleted with the nuclear material at all time points. Smc3 begins to appear in the soluble fraction as cells enter mitosis. Note: the supernatant fractions loaded represent twice as many cell equivalents as the pellet fractions.

teins. Recombinant GST-mp35 was covalently bound to a solid support, and nuclear extracts prepared from asynchronous HeLa cell cultures were cycled over the column for several hours. As a negative control, a parallel column was prepared with bacterially expressed GST and treated with equal amounts of nuclear extract. After a wash step, fractions were eluted from both columns by successively increasing the ionic strength of the wash buffer, and the eluates were then analyzed by SDS-PAGE followed by silver staining. As seen in Figure 4A, only two bands, of apparent molecular weights of ~160 kDa and 145 kDa, eluted specifically from the p35 column (the complete elution series is shown in Figure S1 available online with this article). Both bands were cut from the gel, and proteins within them were identified by liquid chromatography/mass spectrometry. The results are summarized in Table 1. The upper band contained a protein related to Pds5 of *Saccharomyces cerevisiae*, BIMD of *Aspergillus nidulans*, and Spo76 of *Sordaria macrspora*. This human protein was formerly named "androgen-induced prostate proliferative shutoff antigen 3," or AS3, based on its expression under certain conditions (Geck et al., 1999). The lower band contained several proteins, including a second ortholog of *S. cerevisiae* Pds5 (Sumara et al., 2000), as well as the cohesin subunits hSmc1 and hSmc3. All of the proteins positively identified in this experiment play important roles in sister chromatid cohesion or are implicated to do so based on homology to characterized proteins in other systems. Smc1 and Smc3 form a stable heterodimer as part of the cohesin complex, and one of the Pds5 homologs has been shown to interact loosely with this complex (Losada et al., 1998; Sumara et al., 2000). We have named the high molecular weight Pds5 homolog (elsewhere called AS3) hPds5B because of its homology to members of the Pds5 family of proteins and based on the assumption that it interacts with the cohesin proteins identified in this experiment. For clarity, we call the faster migrating protein hPds5A to distinguish it from Pds5B/AS3.

To confirm the nonquantitative results of the mass spectrometry, the eluates were immunoblotted with antibodies against Smc3, Pds5a, and Pds5b/AS3. As seen in Figure 4B, all three proteins were enriched in eluates

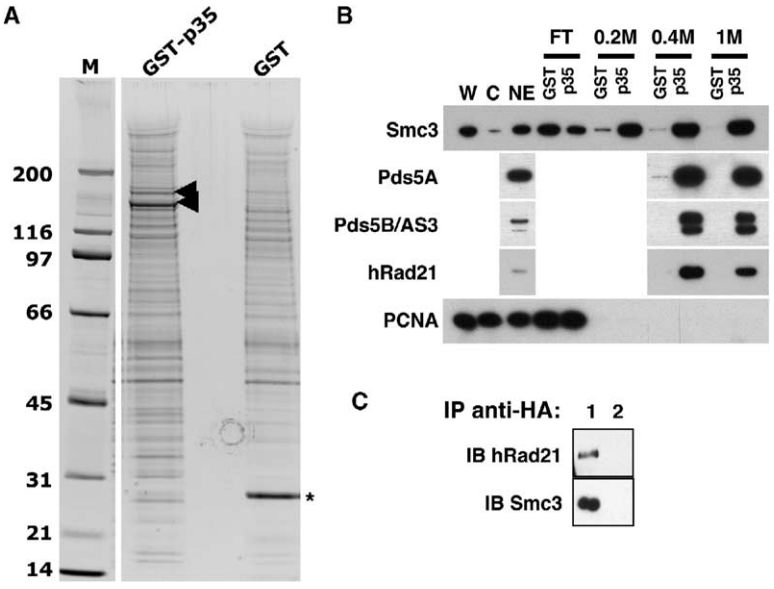

Figure 4. p35 Interacts with Cohesin Proteins

Recombinant GST-p35 was covalently bound to beads that were then used as an affinity matrix to identify interacting proteins from HeLa nuclear extracts.

(A) Shown are the 1 M salt eluates from the GST-p35 column (left) and the GST column (right) run in parallel. Proteins from equal amounts of nuclear extract were allowed to bind to each column. After elution, the samples were TCA precipitated, resolved on a 4%–20% acrylamide gradient gel, and silver stained. Major bands present at ~160 and 145 kDa, indicated by the arrows, are present in the p35 column eluate and not evident in the eluate from the GST column. GST that was not covalently bound to the column began to elute in the high salt washes and is indicated by an asterisk.

(B) Various extracts and fractions from columns described in (A) were immunoblotted for the indicated proteins, including Smc3, Pds5A, Pds5B/AS3, hRad21, and proliferating cell nuclear antigen (PCNA). Abbreviations: W, whole-cell extracts; C, cytosolic fraction; NE, nuclear extract; and FT, flowthrough fractions from the indicated columns. Also shown are the eluates from the salt elutions indicated (0.2, 0.4, and 1 M KCl).

(C) Immunoblot analysis of proteins coprecipitated with p35. 293T cells were transfected with a plasmid encoding either a HA-tagged p35 or an untagged p35, and lysates were prepared. Beads coated with antibodies directed against the HA tag were used to precipitate associated proteins, which were then assayed by immunoblot for the presence of the cohesin subunits Smc3 and Rad21. The cohesin proteins were precipitated specifically from HA-p35-expressing cells (lane 1), but not from p35-expressing cell lysates (lane 2).

from the p35 column when compared to eluates from the GST column. In addition, we blotted for Scc1/Rad21, a non-SMC subunit of cohesin, and found that it was also bound to the p35 beads, although we had not identified it as a band on the silver-stained gel. In contrast, the fractions were not enriched for the presence of PCNA, an abundant nuclear protein, suggesting that the p35 column is not simply "sticky." Together these results suggest that p35 is able to interact with the cohesin complex and its associated proteins.

To confirm the p35-cohesin interaction in vivo, cells were transfected either with a plasmid encoding a tagged version of p35 or an untagged version of the gene. Antibodies directed against the tag were used to immunoprecipitate p35, and the precipitated proteins were analyzed by immunoblot for the presence of both Smc3 and Rad21, subunits of the cohesin complex. As can be seen in Figure 4C, the cohesin subunits associated specifically with the anti-HA beads only when the cells were transfected with HA-tagged p35, consistent with the results obtained by affinity chromatography.

p35 Positively Regulates Sister Chromatid Cohesion

The results of the affinity chromatography experiment described above suggested that p35 might play a role in sister chromatid cohesion. To test this possibility directly, we investigated the effect of p35 levels on chromosome cohesion in an in vitro chromatid cohesion assay in *Xenopus* egg extracts, similar to one described previously (Funabiki and Murray, 2000; Losada et al., 1998). Briefly, sperm nuclei were added to CSF-arrested *Xenopus* egg extracts, and the extracts were released into interphase by the addition of Ca^{2+}. Extracts were programmed by the addition of in vitro-transcribed RNA to express various derivatives of Xp35, illustrated in Figure 5B. These include the wild-type (wt) protein, as well as two different nondegradable derivatives: one containing a mutated KEN box, the other lacking the entire N terminus up to and including the KEN box. In addition, a gene fragment encoding only the N terminus and none of the conserved domains at the C terminus was also tested. After allowing time for replication of the chromosomes, the extracts were driven into mitosis by the addition of fresh cytostatic factor (CSF) extract. Replicated, condensed mitotic chromosomes were fixed in solution and pelleted onto coverslips. The chromosomes were counterstained and observed by epifluorescence microscopy. As seen in Figure 5A, in mock-treated samples, the replicated chromosomes have a characteristic appearance in which sister chromatids

Table 1. Mass Spectrometric Analysis of Proteins Identified by Affinity Chromatography

Apparent Molecular Weight	Protein Identified	Function	Accession Number	Reference
~160	AS3 (hPds5B)	Unknown	AB023196	(Geck et al., 1999)
~145	hSmc3	Sister chromatid cohesion	Q9UQE7	(Losada et al., 2000)
~145	hSmc1	Sister chromatid cohesion/ DNA damage response	I54383	(Losada et al., 2000)
~145	hPds5A	Sister chromatid cohesion	T00374	(Sumara et al., 2000)

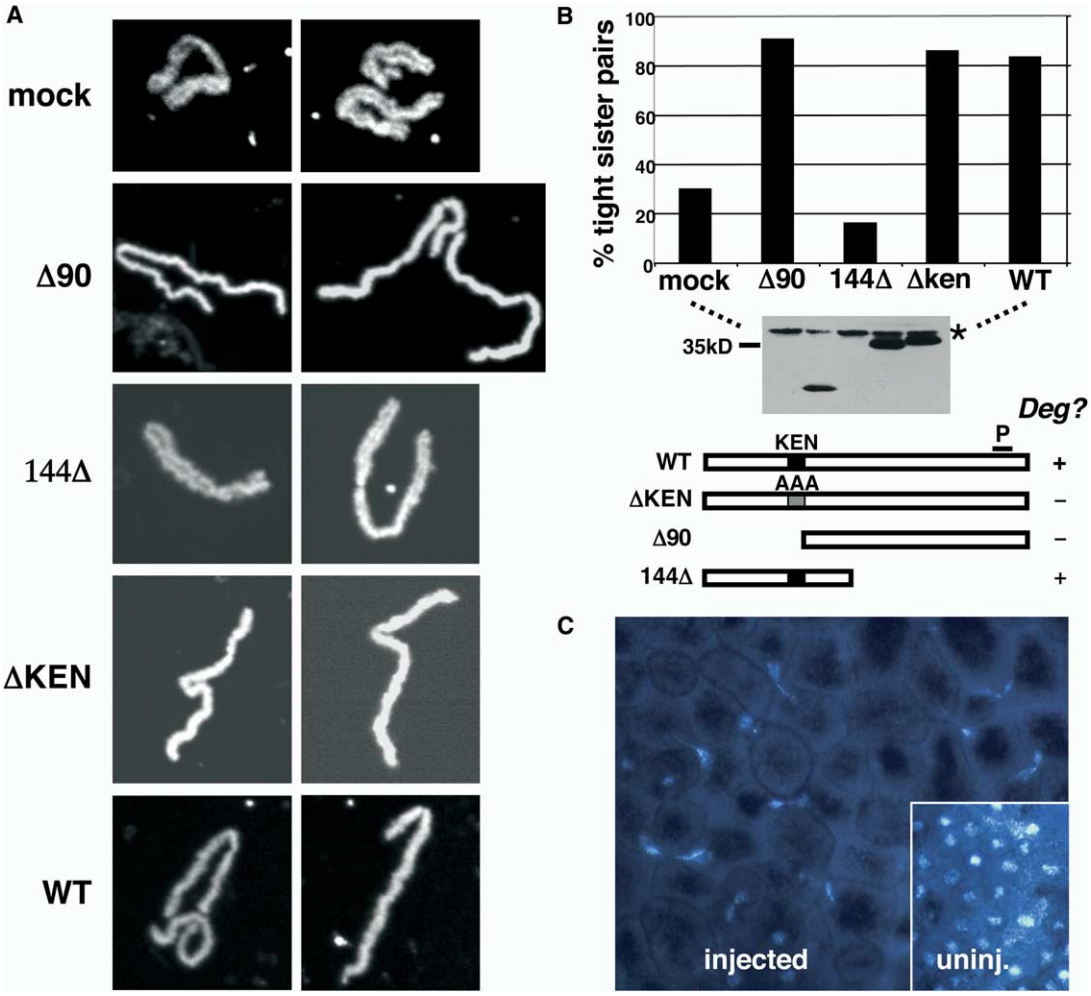

Figure 5. p35 Prevents Sister Chromatid Resolution in *Xenopus* Egg Extracts and Causes a CUT Phenotype in Embyros

(A) Examples from an in vitro chromatid cohesion assay in which mitotic chromosomes were assembled in extracts expressing p35 and derivatives (illustrated graphically in [B]). Sperm nuclei were added to egg extracts expressing derivatives of p35. After DNA replication and entry into mitosis, the mitotic chromosomes were fixed in solution, spun onto coverslips, and stained with DAPI. Examples of unresolved chromatids are seen in extracts expressing wt, KEN mutant, or Δ90 versions of p35. In contrast, both the 144Δ-expressing and mock-treated extracts show normal chromatid resolution.

(B) Quantitation of results in (A) presented as percent-resolved chromatids as a function of the p35 derivative being expressed. Also shown is an immunoblot showing relative expression levels of constructs tested, which are illustrated below the blot. The peptide recognized by the antibody is indicated in the cartoon (P) and thus not present in the 144Δ construct. The asterisk indicates a crossreacting band. An indication whether or not each protein is degraded as an APC^{cdh1} substrate in vitro is shown in the column at the lower right (*Deg?*).

(C) One cell of a two-cell embryo was injected with 0.5 ng of RNA encoding p35, and the embryo was allowed to develop. The image shows a squash of animal pole cells collected at stage 9 from the injected side of an embryo and stained with DAPI to visualize DNA. The autofluorescence of the embryo makes the cellular outlines visible. Some cells have no apparent DNA mass, and others show DNA staining in a bridge between two daughter cells. The inset shows normal cells from the uninjected side of the same embryo (same magnification).

are loosely aligned, both chromatids are easily identifiable, and the kinetochore or "primary constriction" is often apparent. In contrast, the chromosomes in samples to which RNA encoding wt Xp35 or either of two different nondegradable derivatives (ΔKEN and Δ90) had been added showed a strikingly different appearance. In these samples, the sister chromatids were very tightly associated, with little or no gap between them, and the kinetochore region was often more difficult to identify. Several hundred chromosomes from each sample were scored for this sister chromatid resolution phenotype, and the data are summarized in the graph in Figure 5B. The level of expression of p35 obtained by adding RNA to the extracts is much higher than that found endogenously. As can be seen in the immunoblot in Figure 5B, we are in fact unable to detect endogenous protein by immunoblot. Thus, the phenotypes obtained by the addition of RNAs most likely reflect p35 overexpression in this system. The phenotype obtained with the Δ90 version of p35 is indistinguishable from that obtained with the full-length construct, suggesting that the poorly conserved N terminus of the protein is not necessary for the sister chromatid resolution phenotype.

To test how p35 expression affects chromosome segregation, one cell of a two-cell embryo was injected with RNA encoding either wt or nondegradable versions of p35. When embryos were allowed to develop, the injected side appeared normal until approximately stage 9, at which point the cells on the injected side ceased cleaving. When animal cap cells were mechanically removed from the embryo at this stage, squashed, and stained with DAPI, it was possible to see cellular outlines as well as DNA within the cells. As seen in Figure 5C, the cells on the injected side are larger, probably due to cell cycle arrest at the midblastula transition, and show clear defects in DNA segregation. Numerous cells contain no DNA, whereas others show DNA trapped between daughter blastomeres. In contrast, the control cells appear smaller than those on the injected side, and all contain a clear nuclear mass. We do not know the immediate defect that leads to this "CUT" phenotype, but we speculate that it is due to an inability to segregate chromosomes away from each other at anaphase. The absence of both DNA damage and spindle assembly checkpoints in *Xenopus* embryos before the midblastula transition allows cell cleavage despite a failure in anaphase and accumulation of errors until this developmental stage. We have seen no difference between the phenotypes obtained with the KEN box mutant and the wt protein. This is consistent with the observation that there is little or no Cdh1-dependent APC activity in the early embryo, and thus both proteins are stable at this developmental stage. Taken together, the results in Figure 5 indicate that overexpression of p35 in *Xenopus* causes an apparent increase in sister chromatid cohesion and that this defect eventually leads to failures in chromosome segregation.

To confirm that the overcohesion phenotype obtained with p35 overexpression is not due to failures in replication, sperm nuclei were added to extracts supplemented with biotin-labeled dATP, and the same assay was performed. Mitotic chromosomes were then stained with fluorescently labeled avidin to detect incorporation of the labeled nucleotide. In addition, the kinetochores were stained with antibodies to the core kinetochore component CenpA. As can be seen in Figure 6, the chromosomes assembled in extracts with elevated levels of p35 labeled efficiently with streptavidin. In addition, many of the tightly associated chromatids clearly showed double CenpA dots (see inset in Figure 6A), indicating complete centromere replication. Together, these data suggest that the replication is unaffected in samples supplemented with high levels of p35.

Others have shown that conditions that block cohesin removal from the chromatin in prophase result in failures in sister chromatid resolution (Losada et al., 2002). To determine whether excess p35 causes a similar failure to remove cohesin, we stained in vitro-assembled mitotic chromosomes with anti-Smc3 antibodies. Consistent with published reports of cohesin staining on in vitro-assembled chromosomes (Losada et al., 2000), we saw a distinct punctate staining along the length of the sister chromatids. In addition to these speckles, we also saw a diffuse uniform staining of the chromosomes in both control and p35-treated samples, which might represent background staining. As can be seen in Figures 6B and 6C, there was a modest but statistically significant increase in the amount cohesin staining on chromosomes that had been replicated and assembled in the presence of excess p35 when compared to controls.

Cells with Reduced Levels of p35 Arrest in a Prometaphase-like State

The above experiments suggested that p35 is a positive regulator of sister chromatid cohesion. We next wanted to test whether p35 is essential for this process. Because we are unable to detect endogenous p35 in *Xenopus* eggs, we decided to perform loss-of-function experiments in cultured cells in which our antibodies would allow us to assess the success of depletion. Several hp35-derived short hairpin RNAs (shRNAs) were expressed under control of the mouse U6 promoter (Yu et al., 2002) and tested for the ability to decrease p35 levels in vivo. As seen in Figure 7A, one construct, sh6/hp35, was able to reduce significantly the levels of p35 protein when cotransfected into HeLa cells with a plasmid encoding either wt or 6 × Myc-tagged versions of p35. In contrast, the same vector expressing shRNA complementary to the *Xenopus* p35 gene had no obvious effect on expression of the transgene. Because sh6/hp35 is able to dramatically reduce p35 expression from the strong CMV promoter, we reasoned that sh6/hp35 should effectively reduce the endogenous levels of protein, which are considerably lower (see Figure 7A; lanes 1 and 9).

To identify transfected cells and simultaneously to assess any chromosomal defects, HeLa cells were cotransfected with sh6/hp35 and a plasmid expressing a green fluorescent protein-histone H2B gene fusion (GFP-H2B). As seen in Figures 7E and 7F, cells transfected with sh6/hp35 arrested in a prometaphase-like state. These cells had a relatively normal spindle and, although the chromosomes appeared to condense normally, they failed to congress at the spindle midzone. Instead, the chromosomes are dispersed throughout the spindle, with many appearing at or near the spindle poles. As indicated in Figures 7B and 7C, these cells only very rarely form an obvious metaphase plate. In contrast, among control mitotic cells, metaphase figures are the most abundant (see Figure 7C). Consistent with this, there was also an increase in the mitotic index (17% compared to 4.5% in cells transfected with a vector control, measured 70 hr posttransfection), suggesting that the cells were arresting in mitosis or delayed in mitotic exit. We have also tested synthetic siRNA duplexes for depletion of p35 protein from cultured cells and obtained similar results. The phenotype obtained with the shRNA-expressing plasmid was more severe, perhaps due to continuous expression of the shRNA. In an attempt to assess the outcome of the aberrant mitoses in cells with reduced levels of p35, mitotic cells depleted for p35 were filmed for several hours and analyzed in time lapse. The results confirmed that depletion of p35 causes mitotic arrest and showed that this arrest is dynamic. Within a single mitotic cell filmed for more than 3 hr, multiple individual chromosomes were seen to move away from and back toward the spindle midzone (see Supplemental Data for time-lapse movie).

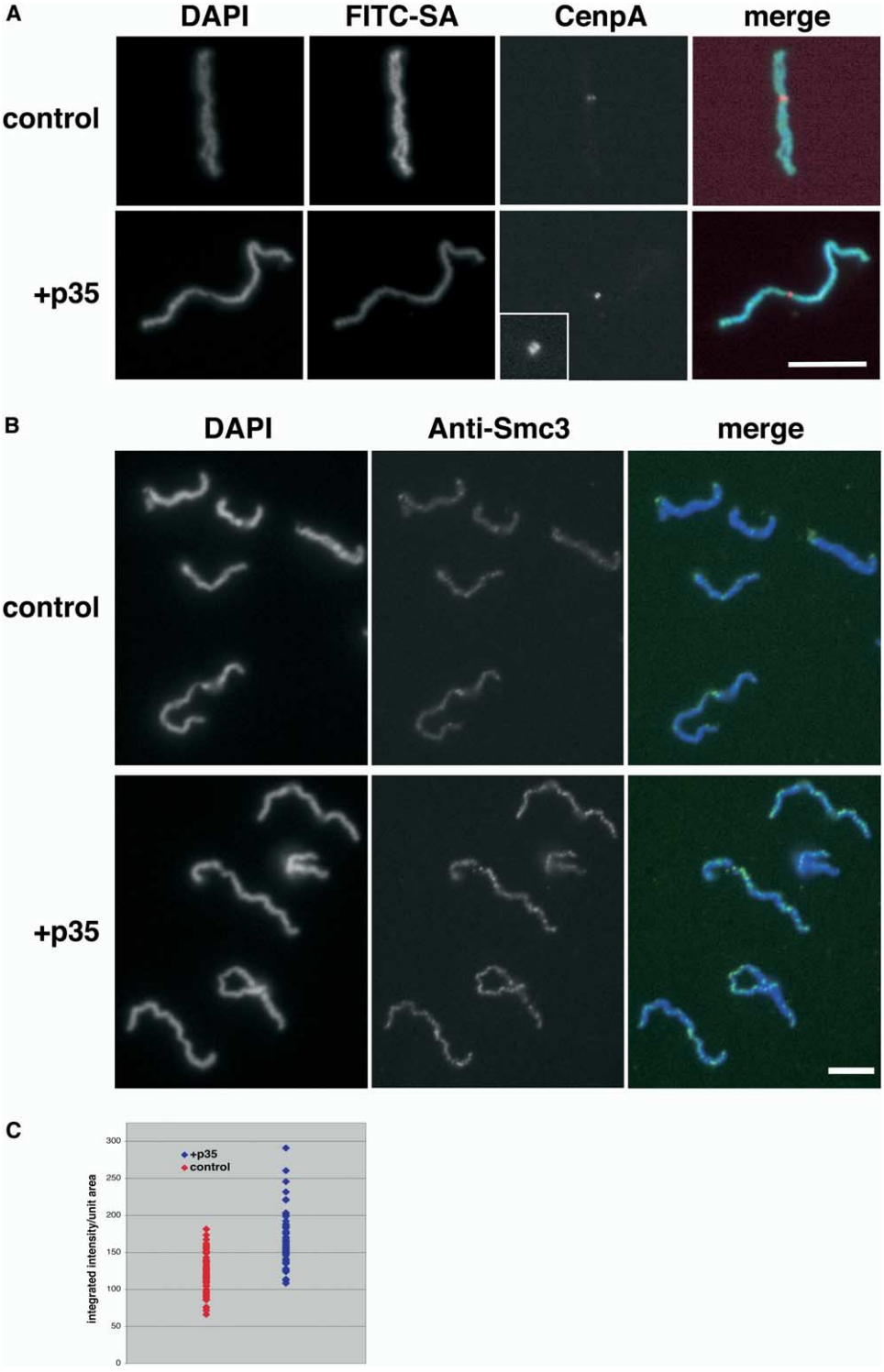

Figure 6. Replication and Cohesin Levels in Unresolved Sister Chromatids

(A) Chromosomes replicated in extracts supplemented with biotin-dATP in the absence (control) or presence (+p35) of recombinant p35 were spun onto coverslips, stained with fluorescein-labeled streptavidin (FITC-SA), immunostained with a labeled anti-CenpA antibody (Cenp-A), and counterstained with DAPI. Inset, 2-fold enlargement of the centromere region from the same sample showing distinct double Cenp-A dots.

(B) Similarly assembled chromosomes were immunostained with anti-Smc3 antibody.

(C) Quantitation of anti-Smc3 staining on individual chromosomes (same experiment as in [B]) reported as integrated fluorescence intensity per unit area. Chromosomes assembled in the presence of exogenous p35 showed a significant increase in Smc3 staining when compared to controls ($p < 0.001$ Student's t test). Bars = 10 μm.

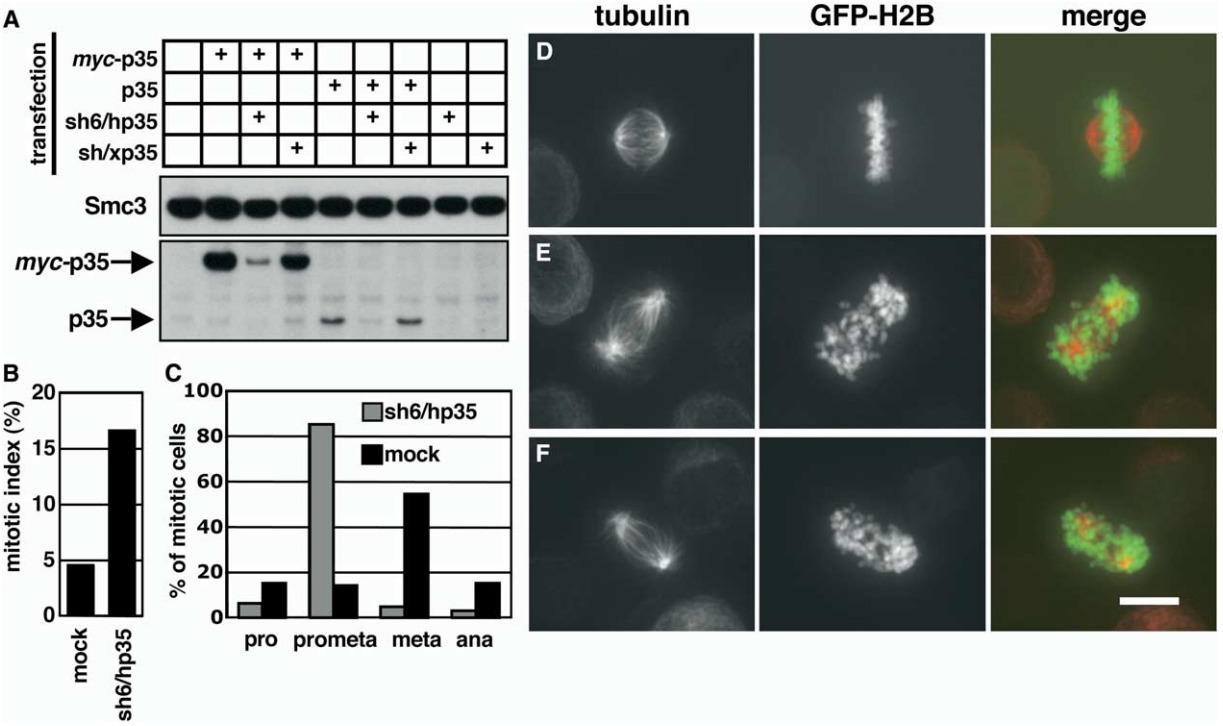

Figure 7. RNAi of p35 Results in Abnormal Mitotic Cells

(A) A plasmid expressing an hp35-derived shRNA, sh6/hp35, is able to reduce levels of p35 expression. HeLa cells were transfected with a plasmid(s) expressing the indicated constructs, and cell lysates were prepared 40 hr posttransfection. The lysates were immunoblotted for p35 protein with antibody 2E10 and for Smc3 as a loading control. sh/xp35: a plasmid similar to sh6/hp35 which instead expresses a shRNA homologous to the *Xenopus* p35 gene. The transfection efficiency in this experiment was ~50% based on a parallel transfection. The blot indicates that sh6/hp35 is able to reduce expression both of wt and Myc-tagged versions of p35 when cotransfected.

(B) Expression of sh6/hp35 results in mitotic arrest. Shown are the mitotic indices in populations of cells transfected with sh6/hp35 or a vector control.

(C) Cells transfected with sh6/hp35 accumulate in a prometaphase-like state. Mitotic cells from populations transfected with either sh6/hp35 or a vector control were categorized for stage of mitosis based on chromosome localization and spindle morphology. Results are presented as percent of total mitotic cells counted.

(D–F) Control cells cotransfected with a plasmid encoding GFP-H2B and an empty RNAi vector assemble normal metaphase figures in which the chromosomes are well organized at the metaphase plate. In contrast, cells cotransfected with sh6/hp35 and a plasmid encoding GFP-H2B show a distinct mitotic phenotype (E and F) in which chromosomes are distributed throughout the spindle and rarely congress to the metaphase plate. Images were collected as a series of confocal images and projected onto a singles plane to show all chromosomes and the entire spindle within each cell. Bar = 10 μm.

In control cells, in contrast, prometaphase cells are more difficult to find and inevitably enter a very tight metaphase within about 60 min of detection (not shown). We reasoned that if the arrest seen in cells depleted for p35 was due to loss of sister chromatid cohesion, then depletion of cohesin proteins should yield the same phenotype. Indeed, when hRad21 was depleted by using siRNAs, the results were indistinguishable from those obtained with p35 depletion (data not shown). The similarity between the results obtained by depleting p35 and by depleting hRad21 suggests that both genes are essential for sister chromatid cohesion.

p35 Is Essential for Sister Chromatid Cohesion

To assess directly the sister chromatid cohesion phenotype of cells depleted for p35, HeLa cells were transfected with sh6/hp35, and chromosome spreads were prepared 40 hr after transfection. All of the spreads shown in Figure 8 were obtained in the absence of microtubule-destabilizing drugs. The mitotic figures in control cells show uniformly paired sister chromatids and overall lower levels of condensation (Figure 8A). In contrast, as shown in Figure 8B, cells expressing the shRNA displayed gross failures in sister chromatid cohesion. In many cells, every chromatid is completely separated from its sister. Occasionally, a few weak associations were seen between chromatids that were possibly sisters. The separated sister chromatids in cells with reduced levels of p35 display a very short and hypercondensed conformation, and most appear crooked or kinked. This is likely due both to sustained mitotic arrest as well as a lack of constraint on condensation normally imposed by association of sister chromatids. As expected, the number of single chromatids in cells depleted for p35 is approximately twice the number of sister chromatid pairs seen in control cells.

To confirm that the failures in sister chromatid cohe-

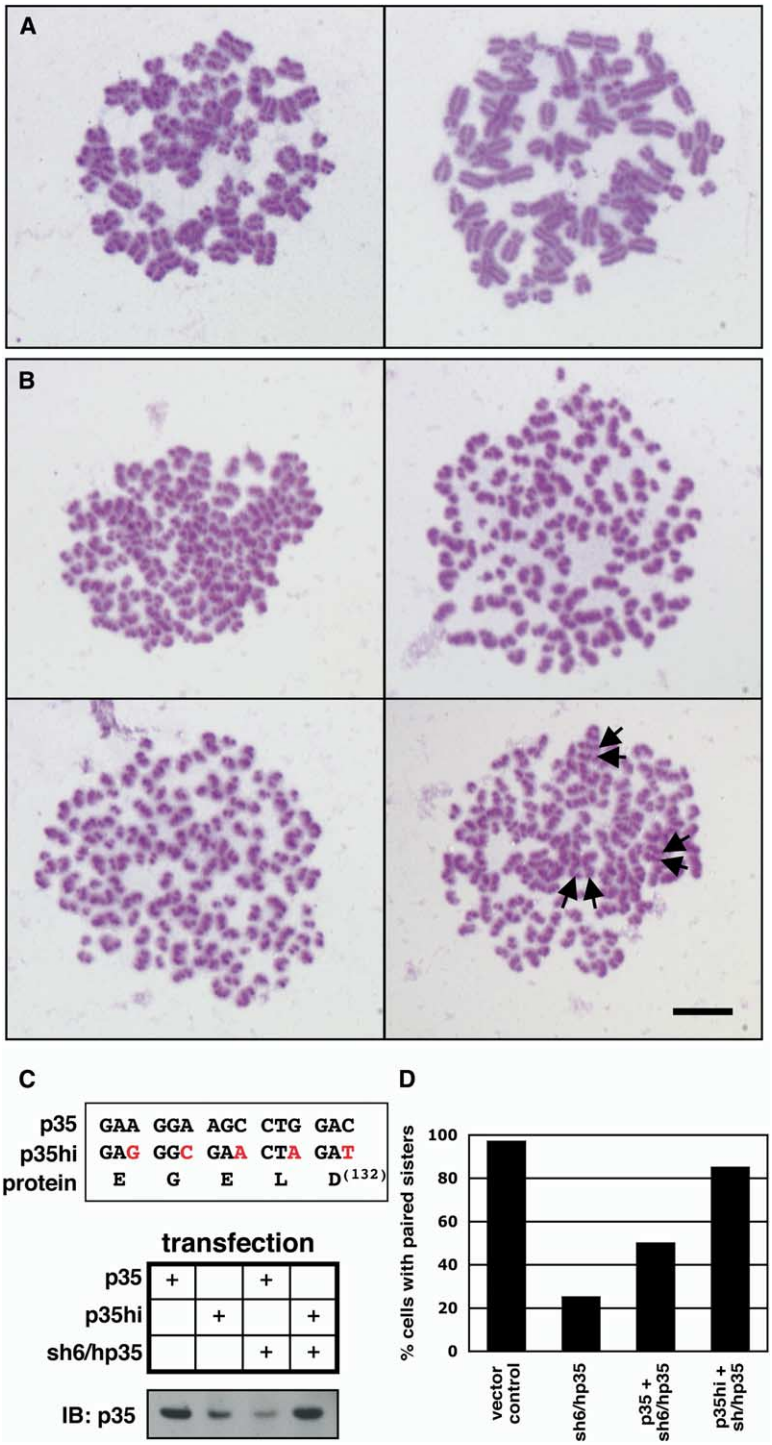

Figure 8. p35 Is Required for Sister Chromatid Cohesion

(A and B) Cells transfected with sh6/hp35 or a control vector were harvested, and Giemsa-stained chromosome spreads were prepared. All spreads were prepared in the absence of microtubule destabilizing drugs. Shown in (A) are spreads from control-transfected cells, which show uniformly paired and associated sister chromatids. In contrast, mitotic spreads from cells transfected with sh6/hp35 (B) showed clear defects in sister chromatid cohesion, as virtually all chromatids are no longer associated with their sisters. Occasionally, weak physical association between what might be sister chromatids can be observed (see arrowheads). Bar = 10 μm.

(C) A plasmid encoding a hairpin-insensitive version of the p35 gene, p35hi, was generated by engineering silent wobble base mutations, indicated in red, at codons 128–132 of the human gene. Lysates from cells transfected with the indicated plasmids were immunoblotted with antibody 2E10 (IB: p35).

(D) Rescue of the sh6/hp35-dependent cohesion defect by expression of p35hi. Cells were transfected with plasmids expressing the indicated constructs, and mitotic spreads were prepared as above and scored for cohesion. Numbers represent the percent of all mitotic cells scored showing a normal cohesion phenotype.

sion were due to reduction in p35 protein levels, we generated a hairpin-insensitive version of the p35 gene (p35hi) and tested the ability of this construct to rescue the knockdown phenotype. Several silent mutations were introduced into the region of the p35 gene targeted by the shRNA, as illustrated in Figure 8C, and a plasmid containing this construct was cotransfected with the shRNA-expressing plasmid (sh6/hp35) into HeLa cells. The mutations result in five mismatches between the shRNA and the transgene, and as shown in the immunoblot at the bottom of Figure 8C, render the transgene insensitive to inactivation by the shRNA based on expression levels. We next tested whether a plasmid containing the p35hi gene could rescue the cohesion defect caused by expression of the shRNA (Figure 8D). As before, transfection of HeLa cells with the shRNA-expressing plasmid resulted in high levels of sister chromatid separation where only 25% of the

mitotic figures show normally paired sister chromatids. This phenotype was partially rescued by coexpression of the wt gene so that 50% of mitotic cells showed normally paired sister chromatids. Finally, rescue of the shRNA effect by cotransfection of the p35hi construct was significantly higher; 85% of the mitotic cells had paired sister chromatids. These results confirm that the failures in cohesion seen in cells expressing the shRNA are in fact due to reduced levels of p35 and not due to nonspecific effects of the shRNA.

One possible explanation for the failure of sister chromatid cohesion in cells lacking p35 is that p35 is required for assembly of the cohesin complex. To test this directly, we have analyzed the sedimentation behavior of cohesin in cells either overexpressing p35 or in cells expressing reduced levels of p35 due to short hairpin interference. We have seen no obvious changes in the sedimentation behavior of the cohesin complex in either condition (see Figures S1A and S1B). We have also seen no obvious change in the localization of cohesin in cells lacking or overexpressing p35 (Figure S1C). Together, these data suggest that p35 might work to regulate the activity of cohesin rather than the assembly or localization of the complex.

Discussion

We have identified a protein, p35, that establishes a connection between sister chromatid cohesion and cell cycle-dependent APC ubiquitin ligase activity. It is an APC^{Cdh1} substrate that acts as a positive regulator of sister chromatid cohesion in cellular extracts and is essential for sister chromatid cohesion in cultured cells. Although p35 is dispersed from the chromatin at the G2/M transition, it is required for sister chromatid cohesion in mitotic cells. We propose calling p35 sororin, from the latin word soror, meaning sister, because of its critical role in sister chromatid cohesion. We have been unable to identify a sororin ortholog in nonvertebrates based on sequence analysis. We suspect that the biochemical function of sororin is fulfilled in other eukaryotes by a gene that does not share obvious homology. We identified sororin in a proteomic screen for APC substrates; because most screens to identify genes involved in the regulation of sister chromatid cohesion have been done in nonvertebrates, this protein was unlikely to be identified by genetic methods.

Sister Chromatid Cohesion and Cell Cycle Progression

Sister chromatid cohesion must be established and dismantled at the appropriate times in the cell cycle to effectively ensure accurate chromosome segregation. It has previously been shown that the activation of APC^{Cdc20} controls the dissolution of cohesion by targeting the anaphase inhibitor securin for degradation. This allows the separase-dependent cleavage of Scc1/Rad21, triggering anaphase. The degradation of most cell cycle substrates of the APC is logical in terms of their function; degradation prevents the untimely presence of activity and in a ratchet-like way promotes cell cycle progression. For example, degradation of cyclin by APC^{Cdc20} paves the way for activation of APC^{Cdh1}, which in turn ensures mitotic exit. In the case of sororin, the reason for its degradation is less obvious. APC^{Cdh1} is active throughout G1, and thus sororin only begins to accumulate in S phase, exactly when cohesion is thought to be established. The cohesin complex itself is known to reload prior to this in telophase, suggesting that sororin might play a role in the establishment step of cohesion. Hypothetically, the timing of sororin degradation through the activation of APC^{Cdh1} might be expected to prevent premature, nonfunctional binding of the cohesin complex in G1, though we have seen no gross mitotic defect in somatic cells expressing nondegradable versions of the protein. The function of sororin may also be redundant with that of other factors that regulate cohesion, with their combined activities ensuring the fidelity of chromosome replication and segregation.

In several systems, abrogation of cohesion by blocking or eliminating Scc1 activity has been shown to result in improper kinetochore assembly, premature sister chromatid separation, and failure to reach metaphase (Guacci et al., 1997; Hoque and Ishikawa, 2002; Sonoda et al., 2001; Vass et al., 2003). We do not yet know the exact nature of the arrest in sororin-depleted cells, although we have evidence that it is Mad2 dependent (not shown) and thus involves activation of the spindle assembly checkpoint (SAC). Whether activation of the SAC in the absence of cohesion is due to the inability of malformed kinetochores properly to attach microtubules and signal their attachment, or due to an inability to generate tension after bipolar attachment to the spindle (because of decreased cohesion between sister chromatids) is not clear.

Cohesin and Sororin

We have shown that recombinant sororin is able to bind cohesin in cellular extracts and that sororin can be used to precipitate cohesin from the cells in which sororin is expressed. Though our results suggest that the affinity between sororin and the cohesin complex is low, it is possible that the interaction is much stronger in the native environment (on the chromosomes) and, in a manner, analogous to certain kinetochore proteins, not easily demonstrated under soluble conditions. We believe that endogenous sororin is bound more tightly to the chromatin than it is to cohesin, making purification of the sororin-cohesin complex technically difficult. The interaction between Pds5 and the core cohesin complex is weak and difficult to maintain in vitro (Sumara et al., 2000; Wang et al., 2002), perhaps for related reasons. Alternatively, sororin might act as a regulator of cohesin function in a way that does not involve high-affinity interactions, as is often seen, for example, in kinase-substrate interactions. We cannot distinguish, at this point, between a model in which sororin is a regulator of cohesin function or a limiting regulatory subunit of the complex. Certainly, we have seen no gross changes in the hydrodynamic properties of cohesin in response to changes in sororin levels, suggesting that sororin does not act to regulate assembly of the cohesin complex.

Among the proteins that were bound to our sororin-affinity resin were two paralogs of Pds5/BIMD/Spo76.

Only one of these proteins has been characterized previously in the context of chromosome architecture and was shown to be loosely associated with the core cohesin complex (Sumara et al., 2000). We assume from our results that in fact both Pds5 paralogs interact with the cohesin complex. Vertebrate cohesin is known to exist in two forms distinct in their Scc3-like subunits (Losada et al., 2000; Sumara et al., 2000), which might also correlate with particular Pds5 proteins. It has recently been demonstrated that a related SMC protein-containing complex, condensin, exists in two forms, which differ in their subunit content and play unique roles in chromosome condensation (Ono et al., 2003).

Cohesion in Embryos and Embryonic Extracts

Mitotic chromosomes assembled in embryonic extracts with elevated levels of sororin stain more intensely for cohesin and show failures in sister chromatid resolution. The apparent overcohesion defect seen in these chromosomes suggests that sororin regulates cohesion either by loading more cohesin in interphase or by preventing the removal of cohesin in prophase or both. Consistent with this, failures in sister chromatid resolution have been seen previously under conditions that prevent cohesin removal from the chromosomes at the G2/M transition (Losada et al., 2002). It is not known what distinguishes the cohesin that remains associated with the chromatin in M phase from the large pool that is removed in prophase. We favor a model in which sororin binds to some limiting site on the chromatin and helps, through its interaction with cohesin, to establish cohesion. Cohesin loading has recently been shown to require licensing of replication (Gillespie and Hirano, 2004; Takahashi et al., 2004). The number of sites of sororin binding on the chromatin might be dependent on the number of licensed origins of replication, perhaps explaining why we see no obvious overcohesion defect in somatic cells with elevated levels of sororin, although we do in embryonic extracts. In embryonic systems, the origins are more closely spaced, allowing complete genome duplication within very rapid cell cycles (Hyrien and Mechali, 1993; Shinomiya and Ina, 1991).

We are unable to detect sororin in *Xenopus* egg extracts. We do not know whether this is because the protein is only expressed at very low levels or whether it reflects a difference between the mechanism of cohesion in pre- and postmidblastula transition embryos. Although sororin ESTs are found in *Xenopus* egg libraries, the lack of Cdh1-dependent APC activity in egg extracts suggests at the very least that sororin activity is unlikely to be regulated by degradation at this developmental stage. If sororin is present in the early embryo, it is possible that mitotic removal of sororin from the chromatin is functionally redundant with Cdh1-dependent degradation, in that both activities effectively inactivate the protein, making Cdh1-dependent degradation unnecessary in the early embryonic divisions.

How Does Sororin Act?

We have shown that sororin is required for sister chromatid cohesion in mitosis and that it can regulate the levels of cohesin associated with mitotic chromosomes. There are several possible models to explain these activities. In the first model, sororin would be required for cohesin to associate with chromosomes. We believe this model is unlikely, as cohesin binds to chromosomes in telophase when sororin levels are low. A second possibility is that sororin acts to regulate the nature of the interaction of cohesin with the chromosomes, thus ensuring cohesion in mitosis. If this were true, then cohesin might associate with chromosomes in cells lacking sororin but would be unable to hold them together. This is consistent with our observation that the pattern of cohesin immunolocalization does not change noticeably in response to changes in sororin levels, nor, in fact, during normal progression from telophase through to G2 (S.R., unpublished data). A final possibility is that sororin acts specifically to ensure mitotic cohesion by preventing prophase removal of cohesin. Sororin might do this indirectly, by marking (in interphase) the cohesin to remain chromosome-associated until metaphase, or directly, with a small pool of sororin (below our limits of detection) remaining chromosome-associated until anaphase. We are currently working to distinguish which among these models is most likely to be true.

Conclusion

One of the most poorly understood aspects of cohesin function has been the mechanism by which cohesion is established. It is possible that sororin will provide insight into this process and as such will be a valuable tool in understanding the regulation of cohesion. Where studied, sister chromatid cohesion has been shown to play critical roles in DNA repair and in proper chromosome partitioning in mitosis. Many tumors result from failures in genome surveillance and display profound defects in the maintenance of proper ploidy. We do not yet know the extent to which failures in the regulation of sister chromatid cohesion contribute to this gross missegregation of chromosomes seen in many tumors. The centrality of sister chromatid cohesion to proper chromosome segregation in model systems, as well as the potential involvement of several cohesion genes in the transformation process (Geck et al., 1999; Ghiselli and Iozzo, 2000; Zou et al., 1999), suggests that a detailed understanding of the mechanism and regulation of sister chromatid cohesion will be useful to our understanding of disease. The identification of a new protein essential for sister chromatid cohesion provides important step forward.

Experimental Procedures

Reagents

Anti-topoIIα antibody was purchased from Stressgen, Inc (Victoria, BC, Canada). Antibodies against hCAPC, Cdc27, cyclin B, cyclin A, and PCNA were purchased from Santa Cruz Biotechnology (Santa Cruz, CA). Anti-Smc3 and anti-hRad21 were purchased from Bethyl Labs (Montgomery, TX). Anti-Nck was purchased from NeoMarkers (Fremont, CA). Cy-3-labeled antitubulin was purchased from Sigma (St. Louis, MO). Anti-AS3 antibody was a generous gift from Ana Soto, whereas anti-hPds5A was generously provided by Jan Michael Peters. Labeled anti-CenpA was kindly provided by Ryoma Ohi. Anti-N-WASP was kindly provided by Henry Ho. Lipofectamine 2000 and TransIT-293 (Mirus, Madison, WI) were used according to

the manufacture's instructions for the transfection of plasmids with serum-free medium (Opti_MEM1, Invitrogen).

Cdh1 Substrate Screen and In Vitro Degradation Assays

The screen was performed exactly as described previously (Ayad et al., 2003). Degradation assays on individual clones were performed as for the screen, only in vitro transcription/translation mix was added at 1:10 to 1:20 (mix:egg extract).

Antibody Production

Rabbit polyclonal anti-p35 antibody was generated against the *Xenopus* p35-derived peptide (C)-DLDEWAAFMNAEFEEA-COOH. The same peptide was then crosslinked to a solid support by using Sulfo-Link Coupling Gel (Pierce, Rockford, IL) and used to affinity purify antibodies from whole serum. For mouse anti-p35 antibodies, mice were injected with a mixture of GST-mp35 and GST-hp35, and monoclonal antibodies were produced according to Harlow and Lane (1988). Monoclonal antibody 2E10 reacted against both human and mouse p35 protein.

Immunofluorescence Microscopy and Immunoblotting

NIH 3T3 cells were grown on poly-L-lysine-coated glass coverslips and fixed with 4% formaldehyde in cytoskeleton buffer (CBS: 10 mM MES [pH 6.1], 138 mM KCl, 3 mM $MgCl_2$, and 2 mM EGTA) containing 0.3% Triton X-100. Cells were washed several times with Tris-buffered saline (TBS: 20 mM Tris HCl, [pH 7.4], and 120 mM NaCl) containing 0.1% Triton X-100. After blocking in antibody-diluting solution (AbDil: TBS, 0.1% TX100, 2%BSA, and 0.1% Sodium azide), cells were incubated in 2E10 diluted in AbDil. Secondary antibodies were obtained from Jackson Immunoresearch (West Grove, PA) and diluted in AbDil. In vitro-assembled chromosomes were spun onto coverslips for immunofluorescence experiments as described (Funabiki and Murray, 2000), and similar incubation conditions were used. For immunoblotting, samples were resolved by SDS-PAGE and transferred to nitrocellulose or PVDF membrane filters. Blots were blocked in TBS containing 0.05% Tween-20 (Bio-Rad) and 4% skim milk powder, and primary and secondary antibodies were diluted in the same solution. Horseradish peroxidase (HRP)-coupled secondary antibodies were used, and Supersignal West Dura (Pierce) was used as a chemiluminescent HRP substrate for all p35 blots. ECL (Amersham) was used in the detection of other antigens.

Cell Culture and Synchronization

All cells were maintained in DMEM supplemented with 10% fetal bovine serum, penicillin, and streptomycin, unless otherwise specified. The HeLa GFP-H2B stable cell line was generously provided by Randall King. For nocodazole arrest and release, cells were grown for 24 hr in media containing 2 mM thymidine, in unsupplemented media for 3 hr, and in media with 100 ng/ml nocodazole for 12 hr. For G1/S synchronization, HeLa S3 cells were grown on dishes in media supplemented with 2 mM thymidine for 16 hr, washed with warm phosphate-buffered saline (PBS), grown in media alone for 6 hr, and then in media supplemented with 2 mM thymidine for an additional 16 hr. Cells were then washed with PBS and transferred to prewarmed media in spinner flasks for the duration of the experiment. Nocodazole (100 ng/ml) was added to the culture 5 hr after release. At the specified time points, cells were removed, washed twice with PBS, washed once with PME (5 mM PIPES [pH 7.2], 5 mM NaCl, 5 mM $MgCl_2$, and 1 mM EGTA) and then swelled for 10 min at 20°C in PME containing 1% thiodiethylene glycol, 10 μg/ml cytochalasin B, 1 μM okadaic acid, and protease inhibitors. Samples were then homogenized 12 times with a dounce homogenizer, nuclei and chromosomes were pelleted at 1000 × g, and supernatants and pellets were mixed with sample buffer.

Chromosome Spreads

Cells were harvested with trypsin and EDTA and resuspended in 50% culture medium: 50% H_20 for 25 min at 20°C. The cells were pelleted by spinning for 5 min at 1000 × g, gently resuspended in a small amount of residual hypotonic medium, and fixed by rapid suspension in ice-cold fix (MeOH:acetic acid; 3:1). After pelleting and resuspending the cells in fresh fix, spreads were prepared by dropping the cell suspension onto clean slides and allowed to air dry. Spreads were stained with Giemsa (Karyomax, Invitrogen) according to the manufacturer's instructions.

Affinity Chromatography

Nuclei were isolated from 5 × 10^8 HeLa-S3 cells by hypotonic lysis and collected by centrifugation at 3700 × g. Nuclear extract was prepared by salt extraction (final concentration 0.6 M KCl in 20 mM HEPES 7.9, 1.5 $MgCl_2$, 0.2 mM EDTA, 0.5 mM DTT, 0.2 mM PMSF, and 25% glycerol). The extract thus obtained was dialyzed against column wash buffer (50 mM HEPES [pH 7.9], 100 mM KCl, 1 mM DTT, 1 mM $MgCl_2$, and 1 mM EGTA) and clarified at 12,000 × g for 20′. GST and GST-mp35 were purified and coupled to agarose beads (Affigel-15, BioRad, Hercules, CA) in 50 mM HEPES, (pH 7.7), and 0.5 M KCl according to the manufacturer's instructions. The beads were washed extensively with 50 mM HEPES (pH 7.7), 1 M KCl, 1 mM $MgCl_2$, and 1 mM DTT and equilibrated with column wash buffer. Nuclear extract was cycled over each column for 3 hr at 4°C, and the columns were then washed with 25 volumes of column wash buffer. Fractions were collected by successive washes of two sequential column volumes each of column wash buffer containing 0.2, 0.3, 0.4, 0.5, and 1.0 molar KCl. The fractions collected were TCA precipitated and analyzed by SDS-PAGE on 4%–20% gradient gels followed by silver stain.

Mass Spectrometry

Protein identification by tandem mass spectrometry was as described (Gygi et al., 1999). Briefly, protein bands were excised from SDS-PAGE gels and digested with sequencing-grade trypsin (Promega, Madison, WI). Digested samples were pressure loaded onto a fused silica microcapillary C18 column (Magic beads, Michrom BioResources, Auburn, CA) packed in house. An Agilent 1100 high-pressure liquid chromatography (HPLC) system (Agilent Technologies) was used to deliver a gradient across a flow splitter to the column. Eluting peptides from the column were ionized by electrospray ionization and analyzed by an LCQ-Deca XP ion-trap mass spectrometer (ThermoFinnigan). Peptide ions were dynamically selected by the operating software for fragmentation. The peptide fragmentation spectra were searched against the NCI human protein database by using the SEQUEST computer algorithm.

In Vitro Chromatid Cohesion Assay

The assay was performed essentially as described in Funabiki and Murray (2000) with the following exceptions. RNA was transcribed from pCS2+-derived vectors using the mMESSAGE mMACHINE In Vitro Transcription Kit (Ambion, Austin, TX). RNAs were eluted in water and added at a 50 ng/ul final concentration to freshly prepared CSF extract. After the addition of 500 sperm nuclei/μl, the extracts were triggered to exit mitosis by the addition of $CaCl_2$ to a final concentration of 0.4 mM. The extracts were incubated at 20°C for 90 min and then were driven back into mitosis by the addition of 0.5 volumes fresh CSF extract. After 90 min, the extracts were diluted into four volumes of chromosome dilution buffer (CDil: 10 mM HEPES [pH 7.6], 200 mM KCl, 0.5 mM $MgCl_2$, 0.5 mM EGTA, and 250 mM sucrose) and incubated for 15 min at 20°C. Samples were then diluted into 4 volumes of freshly prepared fix (20% glycerol, 1× MMR, 0.5% Triton X-100, and 2.7% formaldehyde), spun through a 40% glycerol cushion (in 1× MMR) onto coverslips, and counterstained with 4′,6-diaminidino-2-phenylindole (DAPI).

RNA Interference

Synthetic RNA duplexes were ordered from Dharmacon (Dallas, TX) and transfected into HeLa cells with Oligofectamine (Invitrogen, Valencia, CA) according to the manufacturer's instructions. For Scc1, the sequence targeted was 5′-AACGGACAUCAGGACAUCUCU-3′. For shRNA expression, synthetic DNA oligonucleotides duplexes were cloned into mU6pro as described (Yu et al., 2002). The oligonucleotides used to generate the sh/hp35-6 vector were: 5′-TTTGGAAGGAGAGCTGGACGCCAGAGACACTCTGGCGTCCAGCTCTCCTTCCTTTTT-3′ and 5′-CTAGAAAAAGGAAGGAGAGCTGGACGCCAGAGTGTCTCTGGCGTCCAGCTCTCCTTC-3′. Plasmids were routinely

transfected into HeLa cells by using Lipofectamine 2000 (according to the manufacturer's instructions) using serum-free media (Opti-MEM1, Invitrogen).

Microscopy

For time-lapse analysis, images were collected every 1–2 min by using a Nikon TE2000 with a Perkin Elmer spinning disk confocal system and Solent Scientific incubation chamber. For fixed samples, confocal images were collected by using the same system without incubation. In some experiments, images were collected by using a Zeiss Axiophot 350 and Hamamatsu Orca camera. For color images of chromosome spreads, a Nikon E800 upright microscope was used to collect images with a Hamamatsu C5810 3-Chip Chilled Color Camera. All images were collected by using Metamorph image acquisition and analysis software (Universal Imaging, Downington, PA). Analysis of the levels of cohesin associated with in vitro-assembled chromosomes was performed by measuring the total integrated intensity of cohesin staining and normalizing to the area of DAPI staining for each chromosome. The data are presented as units of integrated intensity per unit area. Similar distributions were obtained when cohesin intensity was normalized to integrated DAPI staining intensity (not shown). In all cases, two background measurements were obtained from each image, and the average background was subtracted from all intensity measurements. Statistical analysis was performed with a t test. $p < 0.001$ that the differences between samples are due to sampling error.

Supplemental Data

Supplemental Data include two figures and one movie and are available online with this article at http://www.molecule.org/cgi/content/full/18/2/185/DC1/.

Acknowledgments

We are deeply indebted to Dean Dawson, Aaron Straight, Randy King, and Johannes Walter for careful review of the manuscript and/or helpful discussions of the data. Assistance in the production of monoclonal antibodies was kindly provided by Annie Yang and other members of the McKeon lab. Michael Rape generously provided samples for the nocodazole release time course. We are grateful to Tersita Bernal for her expert technical assistance with the screen. S.R. was partly supported by a fellowship from the Charles A. King Trust of the Medical Foundation. Additional support came from National Institutes of Health grant GM39023 to M.W.K.

Received: August 31, 2004
Revised: March 4, 2005
Accepted: March 18, 2005
Published: April 14, 2005

References

Ayad, N.G., Rankin, S., Murakami, M., Jebanathirajah, J., Gygi, S., and Kirschner, M.W. (2003). Tome-1, a trigger of mitotic entry, is degraded during G1 via the APC. Cell *113*, 101–113.

Birkenbihl, R.P., and Subramani, S. (1992). Cloning and characterization of rad21 an essential gene of Schizosaccharomyces pombe involved in DNA double-strand-break repair. Nucleic Acids Res. *20*, 6605–6611.

Chan, R.C., Chan, A., Jeon, M., Wu, T.F., Pasqualone, D., Rougvie, A.E., and Meyer, B.J. (2003). Chromosome cohesion is regulated by a clock gene paralogue TIM-1. Nature *424*, 1002–1009.

Ciosk, R., Shirayama, M., Shevchenko, A., Tanaka, T., Toth, A., and Nasmyth, K. (2000). Cohesin's binding to chromosomes depends on a separate complex consisting of Scc2 and Scc4 proteins. Mol. Cell *5*, 243–254.

Fang, G., Yu, H., and Kirschner, M.W. (1998a). The checkpoint protein MAD2 and the mitotic regulator CDC20 form a ternary complex with the anaphase-promoting complex to control anaphase initiation. Genes Dev. *12*, 1871–1883.

Fang, G., Yu, H., and Kirschner, M.W. (1998b). Direct binding of CDC20 protein family members activates the anaphase-promoting complex in mitosis and G1. Mol. Cell *2*, 163–171.

Funabiki, H., and Murray, A.W. (2000). The Xenopus chromokinesin Xkid is essential for metaphase chromosome alignment and must be degraded to allow anaphase chromosome movement. Cell *102*, 411–424.

Geck, P., Szelei, J., Jimenez, J., Sonnenschein, C., and Soto, A.M. (1999). Early gene expression during androgen-induced inhibition of proliferation of prostate cancer cells: a new suppressor candidate on chromosome *13*, in the BRCA2-Rb1 locus. J. Steroid Biochem. Mol. Biol. *68*, 41–50.

Ghiselli, G., and Iozzo, R.V. (2000). Overexpression of bamacan/SMC3 causes transformation. J. Biol. Chem. *275*, 20235–20238.

Gillespie, P.J., and Hirano, T. (2004). Scc2 couples replication licensing to sister chromatid cohesion in Xenopus egg extracts. Curr. Biol. *14*, 1598–1603.

Guacci, V., Koshland, D., and Strunnikov, A. (1997). A direct link between sister chromatid cohesion and chromosome condensation revealed through the analysis of MCD1 in S. cerevisiae. Cell *91*, 47–57.

Gygi, S.P., Rochon, Y., Franza, B.R., and Aebersold, R. (1999). Correlation between protein and mRNA abundance in yeast. Mol. Cell. Biol. *19*, 1720–1730.

Harlow, E., and Lane, D. (1988). Antibodies: A Laboratory Manual (Cold Spring Harbor, NY: Cold Spring Harbor Laboratory).

Hartman, T., Stead, K., Koshland, D., and Guacci, V. (2000). Pds5p is an essential chromosomal protein required for both sister chromatid cohesion and condensation in Saccharomyces cerevisiae. J. Cell Biol. *151*, 613–626.

Hirano, T. (2002). The ABCs of SMC proteins: two-armed ATPases for chromosome condensation, cohesion, and repair. Genes Dev. *16*, 399–414.

Hoque, M.T., and Ishikawa, F. (2002). Cohesin defects lead to premature sister chromatid separation, kinetochore dysfunction, and spindle-assembly checkpoint activation. J. Biol. Chem. *277*, 42306–42314.

Hyrien, O., and Mechali, M. (1993). Chromosomal replication initiates and terminates at random sequences but at regular intervals in the ribosomal DNA of Xenopus early embryos. EMBO J. *12*, 4511–4520.

Ivanov, D., Schleiffer, A., Eisenhaber, F., Mechtler, K., Haering, C.H., and Nasmyth, K. (2002). Eco1 is a novel acetyltransferase that can acetylate proteins involved in cohesion. Curr. Biol. *12*, 323–328.

Kim, S.T., Xu, B., and Kastan, M.B. (2002). Involvement of the cohesin protein, Smc1, in Atm-dependent and independent responses to DNA damage. Genes Dev. *16*, 560–570.

King, R.W., Glotzer, M., and Kirschner, M.W. (1996). Mutagenic analysis of the destruction signal of mitotic cyclins and structural characterization of ubiquitinated intermediates. Mol. Biol. Cell *7*, 1343–1357.

King, R.W., Lustig, K.D., Stukenberg, P.T., McGarry, T.J., and Kirschner, M.W. (1997). Expression cloning in the test tube. Science *277*, 973–974.

Kitagawa, R., Bakkenist, C.J., McKinnon, P.J., and Kastan, M.B. (2004). Phosphorylation of SMC1 is a critical downstream event in the ATM-NBS1-BRCA1 pathway. Genes Dev. *18*, 1423–1438.

Losada, A., Hirano, M., and Hirano, T. (1998). Identification of Xenopus SMC protein complexes required for sister chromatid cohesion. Genes Dev. *12*, 1986–1997.

Losada, A., Yokochi, T., Kobayashi, R., and Hirano, T. (2000). Identification and characterization of SA/Scc3p subunits in the Xenopus and human cohesin complexes. J. Cell Biol. *150*, 405–416.

Losada, A., Hirano, M., and Hirano, T. (2002). Cohesin release is required for sister chromatid resolution, but not for condensin-mediated compaction, at the onset of mitosis. Genes Dev. *16*, 3004–3016.

Lustig, K.D., Stukenberg, P.T., McGarry, T.J., King, R.W., Cryns, V.L., Mead, P.E., Zon, L.I., Yuan, J., and Kirschner, M.W. (1997). Small pool expression screening: identification of genes involved in cell cycle control, apoptosis, and early development. Methods Enzymol. *283*, 83–99.

McGarry, T.J., and Kirschner, M.W. (1998). Geminin, an inhibitor of DNA replication, is degraded during mitosis. Cell *93*, 1043–1053.

Ono, T., Losada, A., Hirano, M., Myers, M.P., Neuwald, A.F., and Hirano, T. (2003). Differential contributions of condensin I and condensin II to mitotic chromosome architecture in vertebrate cells. Cell *115*, 109–121.

Panizza, S., Tanaka, T., Hochwagen, A., Eisenhaber, F., and Nasmyth, K. (2000). Pds5 cooperates with cohesin in maintaining sister chromatid cohesion. Curr. Biol. *10*, 1557–1564.

Pfleger, C.M., and Kirschner, M.W. (2000). The KEN box: an APC recognition signal distinct from the D box targeted by Cdh1. Genes Dev. *14*, 655–665.

Phipps, J., Nasim, A., and Miller, D.R. (1985). Recovery, repair, and mutagenesis in Schizosaccharomyces pombe. Adv. Genet. *23*, 1–72.

Prinz, S., Hwang, E.S., Visintin, R., and Amon, A. (1998). The regulation of Cdc20 proteolysis reveals a role for APC components Cdc23 and Cdc27 during S phase and early mitosis. Curr. Biol. *8*, 750–760.

Reed, S.I. (2003). Ratchets and clocks: the cell cycle, ubiquitylation and protein turnover. Nat. Rev. Mol. Cell Biol. *4*, 855–864.

Shinomiya, T., and Ina, S. (1991). Analysis of chromosomal replicons in early embryos of Drosophila melanogaster by two-dimensional gel electrophoresis. Nucleic Acids Res. *19*, 3935–3941.

Skibbens, R.V., Corson, L.B., Koshland, D., and Hieter, P. (1999). Ctf7p is essential for sister chromatid cohesion and links mitotic chromosome structure to the DNA replication machinery. Genes Dev. *13*, 307–319.

Sonoda, E., Matsusaka, T., Morrison, C., Vagnarelli, P., Hoshi, O., Ushiki, T., Nojima, K., Fukagawa, T., Waizenegger, I.C., Peters, J.M., et al. (2001). Scc1/Rad21/Mcd1 is required for sister chromatid cohesion and kinetochore function in vertebrate cells. Dev. Cell *1*, 759–770.

Stukenberg, P.T., Lustig, K.D., McGarry, T.J., King, R.W., Kuang, J., and Kirschner, M.W. (1997). Systematic identification of mitotic phosphoproteins. Curr. Biol. *7*, 338–348.

Sumara, I., Vorlaufer, E., Gieffers, C., Peters, B.H., and Peters, J.M. (2000). Characterization of vertebrate cohesin complexes and their regulation in prophase. J. Cell Biol. *151*, 749–762.

Takahashi, T.S., Yiu, P., Chou, M.F., Gygi, S., and Walter, J.C. (2004). Recruitment of Xenopus Scc2 and cohesin to chromatin requires the pre-replication complex. Nat. Cell Biol. *6*, 991–996.

Tanaka, T., Fuchs, J., Loidl, J., and Nasmyth, K. (2000). Cohesin ensures bipolar attachment of microtubules to sister centromeres and resists their precocious separation. Nat. Cell Biol. *2*, 492–499.

Toth, A., Ciosk, R., Uhlmann, F., Galova, M., Schleiffer, A., and Nasmyth, K. (1999). Yeast cohesin complex requires a conserved protein, Eco1p(Ctf7), to establish cohesion between sister chromatids during DNA replication. Genes Dev. *13*, 320–333.

Uhlmann, F., and Nasmyth, K. (1998). Cohesion between sister chromatids must be established during DNA replication. Curr. Biol. *8*, 1095–1101.

Uhlmann, F., Lottspeich, F., and Nasmyth, K. (1999). Sister-chromatid separation at anaphase onset is promoted by cleavage of the cohesin subunit Scc1. Nature *400*, 37–42.

Vass, S., Cotterill, S., Valdeolmillos, A.M., Barbero, J.L., Lin, E., Warren, W.D., and Heck, M.M. (2003). Depletion of Drad21/Scc1 in Drosophila cells leads to instability of the cohesin complex and disruption of mitotic progression. Curr. Biol. *13*, 208–218.

Walker, M.G. (2001). Drug target discovery by gene expression analysis: cell cycle genes. Curr. Cancer Drug Targets *1*, 73–83.

Wang, S.W., Read, R.L., and Norbury, C.J. (2002). Fission yeast Pds5 is required for accurate chromosome segregation and for survival after DNA damage or metaphase arrest. J. Cell Sci. *115*, 587–598.

Wang, Z., Castano, I.B., De Las Penas, A., Adams, C., and Christman, M.F. (2000). Pol kappa: a DNA polymerase required for sister chromatid cohesion. Science *289*, 774–779.

Yamamoto, A., Guacci, V., and Koshland, D. (1996). Pds1p is required for faithful execution of anaphase in the yeast, Saccharomyces cerevisiae. J. Cell Biol. *133*, 85–97.

Yazdi, P.T., Wang, Y., Zhao, S., Patel, N., Lee, E.Y., and Qin, J. (2002). SMC1 is a downstream effector in the ATM/NBS1 branch of the human S-phase checkpoint. Genes Dev. *16*, 571–582.

Yu, J.Y., DeRuiter, S.L., and Turner, D.L. (2002). RNA interference by expression of short-interfering RNAs and hairpin RNAs in mammalian cells. Proc. Natl. Acad. Sci. USA *99*, 6047–6052.

Zou, H., McGarry, T.J., Bernal, T., and Kirschner, M.W. (1999). Identification of a vertebrate sister-chromatid separation inhibitor involved in transformation and tumorigenesis. Science *285*, 418–422.

Accession Numbers

The accession number for the *Xenopus* cDNA isolated in the screen is AY963466. A very similar gene is encoded by cDNA found in accession number BC084650.